Reactivating aversive memories in humans: An EEG and Microstates study of post-retrieval processes

Luciano Cavallino[1], Luz Bavassi[1,2], Maria Eugenia Pedreira[1*]

[1] Instituto de Fisiología, Biología Molecular y Neurociencias (IFIBYNE), Laboratorio de Neurociencias de la Memoria, CONICET, Facultad de Ciencias Exactas y Naturales, Universidad de Buenos Aires, Buenos Aires, Argentina (C1428EGA).
[2] Departamento de Física, Universidad de Buenos Aires, Buenos Aires, Argentina

[*] Corresponding author
Maria Eugenia Pedreira, Ph.D. Laboratorio de Neurociencias de la Memoria, Instituto de Fisiología, Biología Molecular y Neurociencias (IFIBYNE, CONICET), Facultad de Ciencias Exactas y Naturales, Universidad de Buenos Aires. Av. Costanera Rafael Obligado, Ciudad Universitaria, Ciudad Autónoma de Buenos Aires, (C1428EGA), Buenos Aires, Argentina. E-mail: mariaepedreira@gmail.com

Running title: Neural markers of post-retrieval threat memory

Keywords: Brain oscillation, EEG, Human, Memory reactivation, Microstates, Threat-conditioning

Abstract

Although fear conditioning is one of the most widely used models to study anxiety in humans, much remains to be explored regarding its underlying neural correlates. In this study, we employed a three-day threat-conditioning protocol in which an angry face (conditioned stimulus, CS+) was paired with an aversive sound (unconditioned stimulus, US). Our main objective was to identify neural markers of post-retrieval processes triggered by the presentation of the CS+ alone, 24 hours after acquisition.

We recorded resting-state electroencephalographic (EEG) activity before and after memory reactivation in two groups of participants (females and males counterbalanced): a Reactivation group previously exposed to threat conditioning on Day 1 (n=26) and a Control group (n=26) with no prior conditioning, focusing on memory-related patterns in the frequency domain and microstate dynamics.

Our results confirmed successful conditioning and memory retention 48 hours later, as evidenced by implicit, declarative, and emotional responses. Regarding neural activity, we found lower beta-band activity (25–30 Hz) in central brain regions after reactivation, which may reflect enhanced post-reactivation processing of the threat conditioning memory, in contrast to participants who viewed the stimulus for the first time. We observed changes in microstates and a potential link between microstate C and conditioned threat memory.

These findings provide initial evidence for neural correlates of post-retrieval processes of an implicit threat memory offering potential relevance for understanding mechanisms implicated in anxiety and related disorders.

Introduction

Understanding environmental threats serves as a critical survival mechanism, allowing organisms to associate previously neutral stimuli with aversive events. This leads to the formation of implicit memories that initiate defensive behaviors, thereby helping to prevent direct harm and enhancing survival rates[1]. However, when an organism fails to suppress threat responses in safe environments, these survival behaviors can become maladaptive, resulting in dysfunctional reactions. Many researchers propose that these mechanisms may contribute to anxiety disorders[2]. In this context, threat-conditioning paradigms offer a powerful experimental approach for investigating the neurobiological foundations of anxiety disorders. Foundational studies in animal models have identified the amygdala as a central hub for the associative learning of neutral cues and aversive outcomes[3–6]. In humans, threat conditioning demonstrates that skin conductance responses are indicative of autonomic nervous system activity[7], acting as a reliable marker for the implicit expression of threat memories, even in the absence of conscious awareness of the underlying contingencies[8–10]. Clinical studies further illustrate that altered threat conditioning and extinction processes are characteristic of anxiety disorders, thus linking fundamental mechanisms of associative learning to psychopathology[11–13]. Collectively, this body of research has established threat conditioning as a cross-species model that connects conserved neural and physiological processes with maladaptive fear and anxiety.

The resurgence of experiments suggesting that specific cues can trigger the reactivation of memories has called into question the longstanding assumption that consolidated memories are permanently resistant to modification[14,15]. This has led to the development of the reconsolidation framework, which posits that the presentation of a reminder triggers reactivation and acts as a mechanism facilitating memory malleability. A closer examination of these protocols reveals that the effectiveness of these reminders relies on the presentation of partial information from the original task. In general, incomplete reminders are characterized by the omission of the expected outcome[16]. However, a deeper analysis of the reminder structures indicates that their effectiveness relies on providing cues that contain critical information, thereby prompting attempts at retrieval[16,17]. Taking this into account, the reactivation of a threat-conditioning memory typically involves reminders in which the unconditioned stimulus (US) is omitted. [14,18]

Anxiety disorders involve physiological, emotional, and cognitive alterations. However, experimental paradigms typically focus on associative responses assessed through autonomic indices (e.g., heart rate variability, skin conductance) and declarative measures (e.g., contingency awareness). This emphasis neglects key components of threat processing, such as cognitive bias, defined as systematic deviations from rational judgment[19,20]. To bridge this gap, we developed a protocol

that integrates physiological and declarative measures with tasks revealing cognitive bias, providing a novel tool to investigate cognitive disturbances associated with anxiety disorders[21]. More recently, we demonstrated that presenting a prediction error reminder (CS+ without US) 24 hours after conditioning led to the labilization of the previously formed memory in a threat conditioning paradigm[22]. This conclusion was based on findings that performing a highly demanding task immediately after memory reactivation eliminated the increased SCR to the CS+ during testing and abolished the cognitive bias effect. These results support the idea that the demanding task weakened the memory trace, but only when the memory had first been reactivated and rendered labile by the reminder.

Given that memory processes rely on neural communication and plasticity across a broad range of timescales, it has been proposed that oscillatory brain activity, ranging from milliseconds to seconds, carries information about higher-order cognitive processes, both in terms of amplitude dynamics and phase coherence[23]. For example, it has been demonstrated that decreases in amplitude within the 8–40 Hz frequency range play an active role in the formation and retrieval of long-term episodic memories[24].

In recent years, the use of Microstate analysis has significantly increased in the search for neural markers associated with various mental processes[25]. Microstates are short-lived, quasi-stable topographies of brain activity (lasting approximately 80–120 ms) that reoccur over time[26,27]. They have been proposed as fundamental building blocks of information processing in the brain[27,28]. Four canonical Microstates were defined based on their topography: Microstate A, B, C, and D[27]. These same Microstates have been consistently identified in a wide range of studies involving different cognitive processes[25], and were also found in the present study. In particular, microstate C activity has been proposed to be related to mind wandering, with decreased activity being linked to externally focused attention[25].

Building on these premises, the present study aimed to identify neural markers associated with the post-reactivation phase of threat-conditioned memories. Employing a three-day threat-conditioning protocol alongside EEG recordings taken during resting states before and after the reminder presentation, we investigated both oscillatory dynamics and Microstate organization to capture the rapid neural processes associated with memory reactivation.

This integrative approach provides new insights into the mechanisms through which reactivated threat memories are stabilized or modified, offering a framework for a deeper understanding of the neural basis of memory reactivation in relation to memory updating. This preliminary evidence suggests that adaptive updating mechanisms may provide new pathways to comprehend why, under certain circumstances, they fail to promote flexible regulation of aversive memories.

Material and methods

Before the experiment, all participants provided written informed consent approved by the Ethics Committee of the Sociedad Argentina de Investigación Clínica (SAIC, Protocol #02/16), in accordance with the Declaration of Helsinki. A total of 52 participants between 18 and 35 years old were included (23 males and 29 females, mean age = 22.92 ± 0.54 years). Three other subjects were excluded from the analysis due to technical problems with the EEG recordings. Participants were randomly assigned to one of two groups: the Control group (15 females and 11 males, 23.03 ± 0.84 years) and the Reactivation group (14 females and 12 males, 22.08 ± 0.70 years).

Subjective Assessment

The State-Trait Anxiety Inventory (STAI-S and STAI-T)[52] and the Beck Anxiety Inventory (BAI)[53] questionnaires were administered to assess participants' anxiety and depressive levels, as these may affect fear conditioning, particularly threat conditioning[54,55]. Participants scoring above STAI > 45 or BAI > 30 were excluded; however, no participants were excluded based on these criteria.

Experimental protocol

Reactivation Group

Participants assigned to the reactivation group completed a three-day consecutive experiment. On Day 1, they performed Stimuli Representation 1 followed by the threat conditioning. Twenty-four hours later (Day 2), a 4-minute resting-state EEG was recorded before stimulus presentation (Rest 1). After the incomplete reminder was presented (CS+ without the tone), a second resting-state EEG was recorded (Rest 2). On Day 3, memory evaluation (Test) was performed, followed by Stimuli Representation 2 (Figure 1). Finally, a Valuation task (probability and cost) was completed.

Control Group

Participants in the control group only completed the Day 2 task: a 4-minute resting-state EEG was recorded before stimulus presentation (Rest 1). After the incomplete reminder was presented, a second resting-state EEG (Rest 2) was recorded (Figure 1).

Cognitive Bias

Stimuli Representation: Participants rated the aversiveness of 12 different male faces (seven angry and five neutral) on a 0–8 scale. Pictures were presented randomly and centrally on a black screen (each measuring 9.5 cm × 7 cm) until a response was given on the keyboard. Stimuli Representation 1 was performed

before conditioning on Day 1, and Stimuli Representation 2 was performed after conditioning on Day 3. Supplementary figure 1

Threat Conditioning

Following a paradigm similar to Picco et al., 2022[22], two aversive (CS+ and CS–) and one neutral (CSn) male faces were presented centrally on a black screen (each slide measuring 9.5 cm × 7 cm) as conditioned stimuli. CS+ and CS– pictures were counterbalanced across participants. The unconditioned stimulus (US) was a 1.5-second auditory tone delivered through stereo headphones, generated by a TG/WN Tone-Noise Generator (Psychlab) and digitally controlled to maintain a mean intensity of 98 dB ± 2 dB. For each participant, US intensity was individually set to evoke an unpleasant but not painful sensation.

Acquisition phase: On Day 1, each face was presented 8 times in a different order (see Supplementary Figure 2). Each trial consisted of a 6-second face presentation followed by a randomly assigned 8–12-second inter-trial interval. The CS+ was paired with the US (tone) on 75% of presentations, overlapping the last 1.5 seconds of the CS. CS– and CSn were never paired with the tone.

Reactivation phase: On Day 2, the CS+ face (previously paired with the tone) was presented as before, but at the time the tone would have occurred, a screen indicating the end of the experiment was shown, and no tone was delivered.

Memory evaluation (Test): On Day 3, one trial of each face (CS+, CS–, CSn) was presented as in the acquisition phase, but without the tone. (Figure 1)

During acquisition and memory evaluation, US expectancy and Skin Conductance Response (SCR) were measured as described below. All faces used in this experiment were taken from the Karolinska Directed Emotional Faces database which is free for research use (database).

Measurements

US Expectancy:
Participants responded “YES” or “NO” using a two-button keyboard, indicating whether they expected the tone to follow the presented face. Responses were considered valid only if made within the first 4.5 seconds post CS presentation (time interval preceding the US presentation).

Implicit Response:

Sympathetic arousal was assessed via the rapid phasic components of electrodermal activity, specifically Skin Conductance Response (SCR), which reflects the emotional and cognitive states triggered by the CS[56].
This involuntary physiological response reflects the level of excitability induced by different stimuli. When a stimulus (CS+) is paired with an aversive stimulus (US), the presentation of the CS+ generates an anticipation of the upcoming US, which increases arousal and may lead to an enhanced SCR. This effect has been previously observed in threat-conditioning studies[21,22,57]. SCR was recorded using a Psychlab Precision Contact Instruments device with a 50 Hz sine excitation voltage (±0.5 V). Two Ag/AgCl electrodes (20 mm × 16 mm) were placed on the intermediate phalanges of the index and middle fingers of the non-dominant hand. A five-point moving average filter was applied to smooth the raw SCR signal.
SCR was calculated as the difference between a baseline (mean conductance during the first 0.5 seconds after CS onset) and the mean conductance between 0.5 and 4.5 seconds post-CS. This time window was selected based on previous studies[7,56]. Each participant thus had one SCR value per trial (27 total: Acquisition: 8 CS+, 8 CS–, 8 CSn; Test –:1 CS+, 1 CS–, 1 CSn). SCR values were standardized into z-scores by subtracting the participant's mean and dividing by the standard deviation.

Outliers in skin conductance responses were removed using an interquartile range (IQR) based criterion. Data were grouped by stimulus type and Trial, and Q1, Q3, and IQR were computed for each group. Observations falling outside the range defined by Q1 − 2×IQR and Q3 + 2×IQR were excluded from further analyses. To perform the repeated-measures ANOVA, two participants were removed from the analysis after outlier removal.

EEG preprocessing

Four minutes of eyes-closed resting-state EEG were recorded for each participant before (Rest 1) and after (Rest 2) stimulus presentation. Given that the most robust results were observed during the last 90 seconds of Rest 1 and the first 90 seconds of Rest 2, this time interval was used for subsequent analyses. EEG was recorded using an Akonic Bio-PC 30 cap-mounted tin electrode system (10/20 international system, Electro-Cap International Inc.), referenced to the average of the two mastoids, sampled at 256 Hz. Data were bandpass-filtered between 1 and 35 Hz (8th-order Butterworth filter) and re-referenced to the average of all channels. Ocular artifacts were removed using independent component analysis (ICA), and erratic or deviating channels were visually inspected and interpolated as necessary. Data were discarded if more than three channels required interpolation, resulting in a total of 26 participants per group after preprocessing.

Time-frequency analysis

Time-frequency decomposition was performed using 7-cycle Morlet wavelets spanning 3-30 Hz. For each participant, the Rest 2 data were baseline-corrected by dividing by the time-averaged Rest 1 data.

Microstate Analysis

Microstate analysis was performed using the Microstate EEGLAB toolbox[29]. After preprocessing (filtering, ICA, interpolation), Rest 1 and Rest 2 data from both groups were combined to generate Microstate prototypes.
The Global Field Power (GFP) was computed at each time point as the standard deviation of the potentials across electrodes, providing a reference-free measure of the overall strength of the scalp electric field. Specifically, GFP was calculated as

$$GFP(t) = \sqrt{\frac{1}{N-1}\sum_{i=1}^{N}\left(V_i(t) - \overline{V}(t)\right)^2} \quad (1)$$

Where N signifies the total number of electrodes (channels), V_i (t) is the voltage recorded at electrode i at time point t, and the average voltage across all electrodes at time point t.

Global Field Power (GFP) was calculated across all channels and frequencies between 1 and 35 Hz after preprocessing. Peaks of local GFP maxima (1000 peaks per participant, minimum 10 ms apart; peaks exceeding 1 standard deviation of GFP values were excluded) were used for clustering. A modified K-means algorithm with 50 random initializations optimized the number of clusters by minimizing the cross-validation criterion CV[29].

$$CV = \hat{\sigma}^2 . \left(\frac{N-1}{N-1-K}\right)^2 \quad (2)$$

Where N signifies the Number of EEG channels, K the number of microstate clusters, $\hat{\sigma}^2$ an estimator of the variance of the residual noise.
Microstates were ordered by decreasing Global Explained Variance (GEV)[29], where the correlation between each EEG sample (x) and its assigned prototype (a) was calculated

$$GEV_n = \frac{\left(Corr(X_n, a_{in}).GFP_n\right)^2}{\sum_{n`}^{N} GFP^2_{n'}} \quad (3)$$

Microstates were labeled according to Tarailis et al., 2024: Microstate C (symmetric anterior-posterior configuration, GEV = 0.26), Microstate A (right frontal-left posterior, GEV = 0.15), Microstate E (posterior-central peak, GEV = 0.14), and Microstate B (left frontal-right posterior, GEV = 0.10). The optimal number of clusters was 4 (CV = 26.4, GEV = 0.64) (Figure 2).

Statistical Analysis

US Expectancy:

Because including the participant as a random effect did not improve model fit, a generalized logistic regression model was used without random effects. Due to quasi-complete or complete separation in some conditions (all participants responding “yes” or “no”), odds ratios of responding “YES” were estimated using Firth’s penalized likelihood method (logistf package in R), which provides bias-reduced estimates and valid inference when standard logistic regression fails. Results are presented as odds ratios (ORs), comparing the probability of responding "yes" to each stimulus with the probability of responding "yes" to the CS+. OR values greater than 1 indicate that the likelihood of a "yes" response to the compared stimulus is higher than to the CS+. In contrast, OR values less than 1 indicate a lower likelihood compared to the CS+.

Implicit Response:

To analyze the effect of stimulus type (CS+, CS–, CSn) on z-scored SCR for each trial, a repeated-measures ANOVA was conducted using R’s base aov function. The error structure accounted for the within-subject design (Error(Participant/stimulus)). Post hoc pairwise comparisons were performed using estimated marginal means (EMMs) with the emmeans package. Model assumptions were checked: residual normality (Shapiro-Wilk test and Q-Q plots), sphericity (Mauchly’s test via afex’s aov_ez function), and homogeneity of variances (Levene’s test from the car package). All assumptions were met (see Supplementary Table 1).

Cognitive Bias:

Ordinal responses (Aversiveness scores) were analyzed using cumulative link mixed models (CLMM) via the ordinal package. Fixed effects included Time (Stimuli Representation 1 vs 2), Stimulus (CSs), and their interaction; participant was included as a random intercept. Estimated marginal means for interactions were computed with emmeans, and pairwise comparisons were adjusted with Tukey’s correction. Assumptions were tested: multicollinearity was assessed via Variance Inflation Factors (VIF < 5 acceptable), and the proportional odds assumption was tested using the nominal_test() function on a model without random effects. (see Supplementary table 2).

EEG Time-Frequency Analysis:

Time-frequency data were compared between Rest 1 and Rest 2 within groups using non-parametric cluster-based permutation tests (FieldTrip toolbox)[58]. Monte Carlo methods with 1000 randomizations controlled for multiple comparisons by clustering electrodes with consistent differences. Two-sided dependent samples t-tests compared Rest 1 vs Rest 2 (cluster alpha = 0.05, minimum two neighboring channels per cluster, significance $p < 0.05$). Data were averaged over time.

Between-group comparisons (Reactivation vs Control, Rest 2 normalized by Rest 1 baseline) were performed using independent t-tests.
Both analyses were conducted on the last 90 seconds of Rest 1 and the first 90 seconds of Rest 2.

Microstate Analysis:

After deriving Microstate prototypes, statistics were calculated per participant, including Global Explained Variance (GEV), Global Field Power (GFP), duration, coverage, and occurrence. After removing outliers, these variables were analyzed per Microstate using linear mixed-effects models with Rest (1 vs 2), Group (Control vs Reactivation), and their interaction as fixed effects, and participant as a random effect. Significant interactions were followed up with post hoc tests using EMMs. Model assumptions (normality and homoscedasticity) were checked via residual diagnostics (Q–Q plots, residuals vs fitted plots). No major deviations were found. Within the Reactivation group, participants were classified into two subgroups using k-means clustering (k = 2) based on standardized differences in evaluative scores and skin conductance responses (CS+ minus CS−) during testing, to compare Microstate measures between subgroups differing in their behavioral responses

Results

US expectancy:

The proportion of "yes" responses (indicating that the US was expected following the CS) was significantly higher for CS+ (Angry face paired with the annoying tone, US) than for CS− (Angry face not paired with the annoying tone) and CSn (Neutral face not paired with the annoying tone) starting from Trial 2 of the acquisition phase. This difference persisted throughout the acquisition phase and into the test phase.

During Trial 1, no significant difference was found in the proportion of "yes" responses to CS+ (46%) versus CS− (30%) (Odds Ratio (OR) = 0.53, 95% CI [0.17, 1.60], $p = 0.26$). However, a higher proportion of "yes" responses was observed for CS+ compared to CSn (0%) (OR = 0.028, 95% CI [0.0002, 0.25], $p < 0.001$).

By the end of the acquisition phase, in Trial 8, a marked difference emerged: 100% of participants responded "yes" to CS+ compared to 0% for both CS− and CSn (OR = 0.00035, 95% CI [0.0000011, 0.0073], $p < 0.001$).

A similar pattern was observed during the memory retention test phase: the proportion of "yes" responses to CS+ was 92%, compared to 7% for CS− (OR = 0.0065, 95% CI [0.0005, 0.041], $p < 0.001$) and 4% for CSn (OR = 0.0038, 95% CI [0.0002, 0.028], $p < 0.001$) (Figure 3a).

Implicit response:

A successful threat conditioning was observed, as evidenced by a greater skin conductance response (SCR) to the CS+ during the late phases of acquisition and the memory retention test, a difference that was not present during the early phases of acquisition (Figure 3b).

To evaluate the implicit response during threat conditioning acquisition, we compared SCR (Z-score) across stimuli (CS+, CS–, and CSn) during the early phase (Trials 1 and 2) and the late phase (Trials 7 and 8). We found that during the early phase, there were no significant differences between stimuli. However, by the end of acquisition, SCR was significantly higher in CS+ than in CS– and CSn, highlighting the effect of conditioning on sympathetic arousal.

Early phase (Trials 1 and 2): The main effect of stimulus was not significant, $F(2, 46) = 2.54$, $p = 0.09$. Figure 3b.

Late phase (Trials 7 and 8). A significant effect of stimulus was found, $F(2, 46) = 5.66$, $p = 0.0063$. Post hoc pairwise comparisons (adjusted for multiple testing): The estimated mean difference between CS1 and CS2 was 0.39 (SE = 0.13), $t(46) = 2.96$, $p = 0.013$; between CS1 and CS3 it was 0.38 (SE = 0.13), $t(46) = 2.86$, $p = 0.016$; and between CS2 and CS3 it was -0.01 (SE = 0.13), $t(46) = -0.09$, $p = 0.995$. Figure 3b.

To evaluate implicit memory retention, we compared SCR (Z-score) across stimuli (CS+, CS–, and CSn) on day 3 (Test). We successfully found memory retention, evidenced by the higher SCR (Z-score) for the CS+ compared with the CS- and CSn. A significant effect of stimulus was found, $F(2, 46) = 4.38$, $p = 0.018$. Post hoc pairwise comparisons (adjusted for multiple testing): The estimated mean difference between CS1 and CS2 was 0.53 (SE = 0.21), $t(46) = 2.53$, $p = 0.038$; between CS1 and CS3 it was 0.54 (SE = 0.21), $t(46) = 2.59$, $p = 0.033$; and between CS2 and CS3 it was 0.01 (SE = 0.21), $t(46) = 0.052$, $p = 0.998$. Figure 3b

Cognitive bias:

To evaluate cognitive bias associated with threat conditioning, we compared the aversiveness scores of the CS+ and CS- before and after conditioning. We found that after conditioning, only the CS+ was rated as more aversive/unpleasant; the aversive score of the CS- did not change, highlighting the effect of the association between that particular image (CS+) and the aversive tone on the aversive perception of the face.

The interaction between Representation (1 and 2) and stimulus (CS+ and CS-) was statistically significant ($\beta = 2.41$, SE = 0.75, $z = 3.19$, $p = 0.001$), suggesting that the effect of stimulus differed by representation. Neither the main effect of Stimulus ($\beta = –0.34$, $p = 0.484$) nor Representation alone ($\beta = –0.86$, $p = 0.095$) reached statistical significance. Meanwhile, no differences were found before and after conditioning for the CS- (Estimate 0.85, SE = 0.51, $z = 1.67$,n=26, $p = 0.339$). The aversiveness

score was higher after conditioning for the CS+ (Estimate = -1.55, SE = 0.52, z = -2.96, n = 26, p = 0.015). Furthermore, the aversiveness score of the representation 2 was higher for the CS+ compared with the CS- (Estimate -2.06, SE = 0.55, z = -3.72, p = 0.001), a difference not found for the representation 1 (Estimate 0.34, SE = 0.49, z = 0.70, p = 0.89). Figure 3c.

Neural correlates:

Time-frequency analysis:

To evaluate changes in brain activity after the stimulus presentation, the power spectrum before (Rest 1) and after (Rest 2) presentation was assessed for all the channels, 3-30 range frequency, and time average (90 seconds).

In both experimental groups we found an increase in activity after the stimulus. Reactivation Group: n=26, p=0.0009 (cluster size of 247 data points). Control Group: n=26, p=0.0009. (cluster size of 371 data points). During Rest 2, the reactivation group showed increased activity across most channels, primarily in the 8–23 Hz frequency range; in the control group, it occurred between 13 and 30 Hz (Figure 4a).

Based on this information, the next step was to compare post-stimulus brain activity (Rest 2, with Rest 1 as baseline) across conditions within the frequency ranges of interest (8–13 Hz and 25–30 Hz), as these bands showed different results across the experimental groups.

An increased oscillatory activity in the control group relative to the reactivation group was identified over central regions in the 25-30 Hz frequency range (n=26, p=0.019, cluster size of 27 data points), Figure 4b. No differences were found for the 8-13 Hz frequency range.

Microstates:

After finding differences in the oscillatory brain activity between the experimental groups in the power spectrum analysis, we aimed to assess the effect on the level of transient changes in neural activity states by conducting a Microstate analysis.

Global Field Power (GFP)

The GFP represents the standard deviation of the voltage amplitude, providing an index of the strength of global activation associated with a given Microstate[25,29]. In the present study, we found higher GFP values during Rest 2 in the control group compared to the reactivation group across all four proposed Microstates.

Pairwise comparisons of estimated marginal means revealed that Control was associated with significantly higher GFP values than Reactivation for Microstates C, A, E and B (Microstate C: estimate = 1.12, SE =0.52, t(58) = 2.14, p = 0.036; Microstate A: estimate = 1.07, SE =0.48, t(57) = 2.23, p = 0.029; Microstate E:

estimate = 1.17, SE =0.52, t(58) = 2.24, p = 0.028; Microstate B: estimate = 1.22, SE =0.43, t(61) = 2.82, p = 0.0065). Figure 5a
No differences were found during Rest 1 (see Supplementary Table 3)

Global Explained Variance (GEV)

The Global Explained Variance (GEV) indicates how well a given prototype explains the data. It is computed as the squared correlation between a sample and its assigned Microstate, weighted by the GFP at that specific time point[25,29]. We found an increase of GEV during Rest 2 only for Microstate C in the Reactivation group (Control group: estimate = -0.011, SE = 0.01, t(48) = -1.12, p = 0.268; Reactivation group: estimate = -0.03, SE =0.01, t(49) = -2.76, p = 0.008). Figure 5b.

Duration

Duration is defined as the average time a given Microstate remains active, expressed in milliseconds[25,29]. Significant differences were found only for Microstate A, with the Reactivation group showing longer durations during Rest 2, a difference that was not observed during Rest 1 (Rest1: estimate = -4.49, SE = 3.02, t(73) = -1.48, p = 0.141; Rest 2: estimate = -8.5, SE =3, t(72) = -2.83, p = 0.006). Figure 5c

Coverage

Coverage is defined as the fraction of time a given Microstate remains active[25,29]. Significant differences were found only for Microstate E, with the Reactivation group showing a lower coverage during Rest 2 compared with Control group, a difference that was not observed during Rest 1 (Rest1: estimate = 0.042, SE = 0.026, t(59) = 1.64, p = 0.105; Rest 2: estimate = 0.052, SE =0.026, t(58) = 2.03, p = 0.046). Figure 5d

Occurrence

Occurrence reflects the average number of times per second a Microstate is dominant[25,29]. We found a decreased occurrence during Rest 2 only for Microstate E in the Control group (Control group: estimate = 0.19, SE = 0.086, t(50) = 2.22, p = 0.03; Reactivation group: estimate = 0.155, SE =0.084, t(49) = 1.83, p = 0.072). Figure 5e.
Results from the other Microstates were present in supplementary table 4.

Relation between memory retention measures and brain activity

To evaluate whether brain activity differed according to responses to stimuli during the memory test, participants in the Reactivation group were divided into two subgroups based on behavioral variables: stimulus representation and SCR. Participants were clustered into two groups: one subgroup characterized as “good learners,” who showed an increased aversiveness score for the CS+ after conditioning and/or a greater SCR to the CS+ than to the CS– (Cluster 2), and

another subgroup characterized as “poor learners,” who did not show an increase in CS+ aversiveness and/or did not exhibit a greater SCR to the CS+ (Cluster 1). Figure 6a

Power
As all assumptions were met (Shapiro–Wilk: $p = 0.509$; Levene’s test: $p = 0.385$), a linear model was performed to compare the power in Rest2, using Rest1 as baseline (25–30 Hz, averaged over time and restricted to the significant channel identified in Figure 4C). Poor learners showed greater power than good learners ($t(22) = 2.10$, $p = 0.047$). Figure 6b.

Microstate C
GEV increased after the reminder in good learners only, with no change observed in poor learners (poor learners: estimate = -0.028, SE = 0.022, $t(23) = -1.3$, $p = 0.20$; Good learners: estimate = -0.064, SE =0.024, $t(24) = -2.58$, $p = 0.016$). Figure 6c.

We found lower beta activity in the Reactivation group and an increased GEV for Microstate C (Figures 4 and 5). Similar results were observed when comparing the good learners subgroup with the poor learners subgroup, with the latter showing a pattern more similar to the Control group. We also found group differences in GFP that support these findings (Supplementary Table 5).

Discussion

Adaptive behavior requires not only the detection of environmental threats but also the updating of previously acquired information. Memory reactivation facilitates this flexibility by making consolidated memories labile, allowing for modification through reconsolidation[14,17].

The present study aimed to identify neural markers of the post-reactivation process of a threat-conditioning memory. We recorded EEG activity before and after reminder presentation in two groups: one that had undergone training (the Reactivation group) and another that had not (the Control group). We found a reduction in beta-band activity (25–30 Hz) in central brain regions and changes in the characteristics of microstate C after memory reactivation, which we therefore propose as neural markers of a post-retrieval process in a threat-conditioning memory.

As previously noted, the amplitude of brain oscillations can provide valuable insights into complex mental processes, with specific oscillatory frequencies associated with particular functions[23,30]. For instance, Zhu and colleagues utilized MEG to demonstrate a decrease in beta-band activity (15–25 Hz) during the reactivation of episodic memory[31]. Likewise, Griffiths and coworkers presented fMRI/EEG evidence suggesting that reductions in alpha/beta activity (8–30 Hz) are associated with

enhanced information processing in associative memories[32]. These findings align with the desynchronization hypothesis, which underscores the importance of decreased 8–30 Hz activity during both memory encoding and retrieval[24]. According to this hypothesis, desynchronization is linked to a more nuanced representation of information, thereby facilitating both encoding and retrieval. Based on working memory studies in primates, Miller and colleagues have suggested that a decrease in alpha/beta activity may provide a framework for determining which brain regions are available or unavailable for activation, thereby regulating activity at other frequencies, such as the gamma band[33–35].

In line with this framework, we found reduced beta activity (25–30 Hz) in the Reactivation group compared to the Control group, which could reflect greater post-reactivation processing of the memory, as opposed to participants without prior knowledge of the stimuli. Furthermore, considering that the image presented to the Reactivation group was previously paired with an aversive sound and could therefore trigger the recall of a threatening situation, the observed beta reduction is consistent with MEG results by Roxburgh and coworkers, who reported a decrease in the 14–30 Hz frequency band during periods of threat (unexpectedly delivered electric shocks)[36].

Regarding alpha activity (8–13 Hz), we observed an increase in the Reactivation group that was absent in the Control group. However, no significant differences emerged between the two groups. Previous research has suggested that increases in alpha activity are linked to inhibition. Specifically, it has been proposed that regions engaged in a task exhibit decreased alpha activity. In contrast, non-involved regions display increased alpha, thereby inhibiting potential interference and directing attentional resources[37]. In episodic memory interference paradigms, an increase in alpha/beta activity (11.5–20 Hz) has been observed in competing memory regions during retrieval, implying that such increases serve to inhibit interference from competing memories[38]. Given this evidence, the alpha increase seen in the Reactivation group may indicate an inhibition of interference with the reactivated memory. However, due to the lack of significant group differences, we cannot draw strong conclusions.

It is worth noting that many studies report decreases in alpha/beta and beta at the time of reactivation, mainly in episodic or working memory paradigms[24,39]. In contrast, our study assessed activity during 90-second resting-state intervals, which may reflect not only reactivation itself but also subsequent post-reactivation processes, specifically in the context of threat-conditioning memories.

EEG activity can be described as a dynamic system, with Microstates reflecting brief, stable topographies of electrical activity across the scalp. Resting-state EEG, widely used in clinical research, captures spontaneous neural dynamics that may reveal how large-scale brain networks operate[40–42]. Building on our spectral analysis of resting-state activity, we complemented this approach with Microstate analysis.

Four canonical Microstates (A–D) have been consistently described across a wide range of studies and cognitive domains, supporting their role as fundamental units of brain activity[27]. In line with this literature, we also identified these canonical Microstates in our data (Microstate D sometimes appears as an inverse topography with a posterior-central peak, as in the present work. Nevertheless, following the labels from Tarailis et al. (2024)[25], we label these inverted Microstates as E). While Microstate analysis has been increasingly applied in psychiatric and neurological disorders, comparatively fewer studies have examined how these patterns relate to specific cognitive processes. In the present study, we aim to contribute evidence on Microstate dynamics following the reactivation of threat memories.

Microstate A has been primarily associated with auditory and visual processing; however, some evidence suggests it may also be linked to arousal[25]. Antonova and coworkers found a positive correlation between Microstate A duration and self-reported alertness during task performance, which also correlated with increased alpha activity (8–12 Hz)[43]. Consistent with this evidence, we found greater Microstate A duration in the Reactivation group, possibly reflecting a higher state of alertness due to the association between the CS+ and the aversive US.

Microstate E has been associated with emotional information processing and alertness[25,44]. In particular, its coverage has been negatively correlated with somatic awareness[45,46]. In our study, we found reduced Microstate E coverage in the Reactivation group, which may also reflect heightened alertness due to anticipation of the aversive sound. However, because the occurrence decreased only in the Control group, the effect of reactivation on Microstate E should be interpreted with caution.

Given that Microstate C accounts for the most significant proportion of total variance, we focused our analysis of behavioral correlations on this Microstate. Based on fMRI, EEG, and brain stimulation evidence, Microstate C has been proposed to reflect the default mode network (DMN)[25,47,48] . The DMN is a network of interconnected brain regions, whose decreased activity has been linked to externally focused attention, whereas it is typically active during mind wandering or resting states[41,49,50].

In our study, GFP was greater in the Control group across microstates. In particular, the reduced Microstate C activity observed in the Reactivation group may reflect increased attentional engagement with a salient stimulus. In contrast, the greater activity in the Control group may reflect mind wandering following the presentation of a stimulus without associated information. We also found that GEV increased after stimulus presentation only in the Reactivation group.

Interestingly, when we further subdivided the Reactivation group into two clusters based on their physiological responses (SCR) and cognitive biases, we identified “good learners” (those showing stronger CS+ than CS– responses after conditioning) and “poor learners” (those showing weaker or absent effects). In this case, GEV increased only in the good learners. We propose that, for good learners, the CS+ stimulus was likely more salient; in contrast, for poor learners, the CS+ was likely less salient, leading to brain activity patterns more similar to those of the Control group, for whom the CS+ carried no relevant information. These findings are further supported by the GFP analysis: poor learners showed increased post-stimulus GFP in Microstate C, possibly reflecting mind wandering, whereas good learners did not, consistent with a greater focus on the stimulus. Moreover, when comparing EEG power between these two subgroups, we found higher power in poor learners (averaged over the 25–30 Hz range and across the previously identified significant channels), similar to the lower beta activity observed in the Control group. This analysis allows us to evaluate differences in Microstates and power between groups separated by behavior, not only through implicit responses but also by incorporating cognitive biases.

We confirmed the successful conditioning and memory retention of our protocol through implicit and declarative responses, along with the associated cognitive biases. In particular, the CS+ stimulus (paired with an aversive tone, US) elicited greater skin conductance responses and higher aversiveness ratings compared to non-reinforced stimuli. These findings indicate that threat conditioning engages both physiological and cognitive responses, providing a solid framework for investigating how memory-updating mechanisms may facilitate or hinder the flexible regulation of aversive memories.

Previous results[22] also demonstrated that presenting a reminder containing a prediction error 24 hours after acquisition induces memory labilization. Picco and colleagues found that when participants performed a high-demand cognitive task after a reminder presentation (CS+ without US), memory retention was weakened[22]. This effect was explained by competition for cognitive resources required for both the reconsolidation of the reactivated memory and the demanding task, ultimately weakening memory. By contrast, when participants performed a low-demand task after reactivation, no such memory impairment was observed. In line with these results, de Voogd and colleagues found that participants exposed to a working memory task showed reduced threat responses and enhanced extinction learning, which could be explained by competition between the salience and central executive networks of the brain[51]. These results confirm that the incomplete reminder used in this protocol elicits the reactivation of the conditioned memory.

Taken together, our results suggest that beta-band activity (25–30 Hz) in central regions and microstate C plays a crucial role in the post-reactivation processes of

threat-conditioning memories. Furthermore, Microstate A appeared to be active for a longer duration following memory reactivation, and we propose a potential role for Microstate E. However, further studies are needed to clarify this. Finally, we suggest that the Microstate C pattern observed in the Control group reflects periods of mind wandering. In contrast, the association between this microstate and behavioral outcomes indicates that the reminder was more salient for participants who showed clearer evidence of learning and memory retention.

Limitation: While our primary objective was to focus on the reactivation of threat memories, we cannot entirely rule out the possibility that episodic retrieval played a role, as the similarity of contexts across sessions might have prompted recall of the prior visit. This overlap could have influenced the neural patterns we observed. However, it is crucial to emphasize that the resting-state recordings were collected immediately following the presentation of the reminder cue. For the Reactivation group, this cue served as an implicit memory trigger, while for the Control group, it functioned as a neutral, meaningless stimulus. Despite the potential influence of episodic factors, the significant between-group differences in beta-band activity and microstate dynamics offer convergent evidence for distinct post-retrieval processes, reinforcing the notion that threat memories remain malleable even after reactivation.

Acknowledgments

This work was supported by a grant from the University of Buenos Aires UBACYT 2023 (20020220400164BA) and CONICET PIP 2021-2023.

Author Contributions: L.B and M.E.P designed research; L.C performed research and analyzed data; L.B, M.E.P and L.C wrote the paper.

Competing interests: The authors declare no competing interests.

Reference

1. Fanselow, M. S. The role of learning in threat imminence and defensive behaviors. *Curr. Opin. Behav. Sci.* **24**, 44–49 (2018).

2. Grupe, D. W. & Nitschke, J. B. Uncertainty and anticipation in anxiety: an integrated neurobiological and psychological perspective. *Nat. Rev. Neurosci.* **14**, 488–501 (2013).

3. LeDoux, J. E. Cognitive-emotional interactions. *Cogn. Neurosci. Emot.* 129–155 (2000).

4. Davis, M. The role of the amygdala in fear and anxiety. *Annu. Rev. Neurosci.* **15**, 353–375 (1992).

5. Rogan, M. T., Stäubli, U. V. & LeDoux, J. E. Fear conditioning induces associative long-term potentiation in the amygdala. *Nature* **390**, 604–607 (1997).

6. Fanselow, M. S. & Poulos, A. M. The neuroscience of mammalian associative learning. *Annu. Rev. Psychol.* **56**, 207–234 (2005).

7. Sjouwerman, R. & Lonsdorf, T. B. Latency of skin conductance responses across stimulus modalities. *Psychophysiology* **56**, e13307 (2019).

8. Öhman, A. & Mineka, S. Fears, phobias, and preparedness: Toward an evolved module of fear and fear learning. *Psychol. Rev.* **108**, 483–522 (2001).

9. Phelps, E. A. & LeDoux, J. E. Contributions of the Amygdala to Emotion Processing: From Animal Models to Human Behavior. *Neuron* **48**, 175–187 (2005).

10. Raio, C. M., Carmel, D., Carrasco, M. & Phelps, E. A. Nonconscious fear is quickly acquired but swiftly forgotten. *Curr. Biol.* **22**, R477–R479 (2012).

11. Grillon, C. Startle reactivity and anxiety disorders: aversive conditioning, context, and neurobiology. *Biol. Psychiatry* **52**, 958–975 (2002).

12. Lissek, S. *et al.* Classical fear conditioning in the anxiety disorders: a meta-analysis. *Behav. Res. Ther.* **43**, 1391–1424 (2005).

13. Milad, M. R. & Quirk, G. J. Fear Extinction as a Model for Translational Neuroscience: Ten Years of Progress. *Annu. Rev. Psychol.* **63**, 129–151 (2012).

14. Nader, K., Schafe, G. E. & Le Doux, J. E. Fear memories require protein synthesis in the amygdala for reconsolidation after retrieval. *Nature* **406**, 722–726 (2000).

15. Alberini, C. M. Mechanisms of memory stabilization: are consolidation and reconsolidation similar or distinct processes? *Trends Neurosci.* **28**, 51–56 (2005).

16. Forcato, C., Argibay, P. F., Pedreira, M. E. & Maldonado, H. Human reconsolidation does not always occur when a memory is retrieved: The relevance of the reminder structure. *Neurobiol. Learn. Mem.* **91**, 50–57 (2009).

17. Fernández, R. S., Boccia, M. M. & Pedreira, M. E. The fate of memory: Reconsolidation and the case of Prediction Error. *Neurosci. Biobehav. Rev.* **68**, 423–441 (2016).

18. Kindt, M., Soeter, M. & Vervliet, B. Beyond extinction: erasing human fear responses and preventing the return of fear. *Nat. Neurosci.* **12**, 256–258 (2009).

19. Tversky, A. & Kahneman, D. Judgment under Uncertainty: Heuristics and Biases: Biases in judgments reveal some heuristics of thinking under uncertainty. *Science* **185**, 1124–1131 (1974).

20. Leung, C. J., Yiend, J., Trotta, A. & Lee, T. M. C. The combined cognitive bias hypothesis in anxiety: A systematic review and meta-analysis. *J. Anxiety Disord.* **89**, 102575 (2022).

21. Fernández, R. S., Picco, S., Messore, F. & Pedreira, M. E. Effects of Threat Conditioning on the Negative Valanced Systems and Cognitive Systems. *Sci. Rep.* **8**, 11221 (2018).

22. Picco, S., Bavassi, L., Fernández, R. S. & Pedreira, M. E. Highly Demand Working Memory Intervention Weakens a Reactivated Threat Memory and the Associated Cognitive Biases. *Neuroscience* **497**, 257–270 (2022).

23. Lakatos, P. *et al.* An Oscillatory Hierarchy Controlling Neuronal Excitability and Stimulus Processing in the Auditory Cortex. *J. Neurophysiol.* **94**, 1904–1911 (2005).

24. Hanslmayr, S., Staudigl, T. & Fellner, M.-C. Oscillatory power decreases and long-term memory: the information via desynchronization hypothesis. *Front. Hum. Neurosci.* **6**, (2012).

25. Tarailis, P., Koenig, T., Michel, C. M. & Griškova-Bulanova, I. The Functional Aspects of Resting EEG Microstates: A Systematic Review. *Brain Topogr.* **37**, 181–217 (2024).

26. Lehmann, D., Ozaki, H. & Pal, I. EEG alpha map series: brain micro-states by space-oriented adaptive segmentation. *Electroencephalogr. Clin. Neurophysiol.* **67**, 271–288 (1987).

27. Koenig, T. *et al.* Millisecond by Millisecond, Year by Year: Normative EEG Microstates and Developmental Stages. *NeuroImage* **16**, 41–48 (2002).

28. Lehmann, D. Brain Electric Microstates and Cognition: The Atoms of Thought. in *Machinery of the Mind: Data, Theory, and Speculations About Higher Brain Function* (eds John, E. R., Harmony, T., Prichep, L. S., Valdés-Sosa, M. & Valdés-Sosa, P. A.) 209–224 (Birkhäuser, Boston, MA, 1990). doi:10.1007/978-1-4757-1083-0_10.

29. Poulsen, A. T., Pedroni, A., Langer, N. & Hansen, L. K. Microstate EEGlab toolbox: An introductory guide. Preprint at https://doi.org/10.1101/289850 (2018).

30. Klimesch, W. The frequency architecture of brain and brain body oscillations: an analysis. *Eur. J. Neurosci.* **48**, 2431–2453 (2018).

31. Zhu, Z., Wang, Y., Jia, J. & Wu, Y. Beta and alpha desynchronizations underlie reconsolidation-mediated episodic memory updating. *Neuropsychologia* **132**, 107135 (2019).

32. Griffiths, B. J. *et al.* Alpha/beta power decreases track the fidelity of stimulus-specific information. *eLife* **8**, e49562 (2019).

33. Miller, E. K., Lundqvist, M. & Bastos, A. M. Working Memory 2.0. *Neuron* **100**, 463–475 (2018).

34. Lundqvist, M., Herman, P., Warden, M. R., Brincat, S. L. & Miller, E. K. Gamma and beta bursts during working memory readout suggest roles in its volitional control. *Nat. Commun.* **9**, 394 (2018).

35. Mendoza-Halliday, D. *et al.* A ubiquitous spectrolaminar motif of local field potential power across the primate cortex. *Nat. Neurosci.* **27**, 547–560 (2024).

36. Roxburgh, A. D., White, D. J., Grillon, C. & Cornwell, B. R. A neural oscillatory signature of sustained anxiety. *Cogn. Affect. Behav. Neurosci.* **23**, 1534–1544 (2023).

37. Klimesch, W. Alpha-band oscillations, attention, and controlled access to stored information. *Trends Cogn. Sci.* **16**, 606–617 (2012).

38. Waldhauser, G. T., Johansson, M. & Hanslmayr, S. Alpha/Beta Oscillations Indicate Inhibition of Interfering Visual Memories. *J. Neurosci.* **32**, 1953–1961 (2012).

39. Griffiths, B. J., Martín-Buro, M. C., Staresina, B. P., Hanslmayr, S. & Staudigl, T. Alpha/beta power decreases during episodic memory formation predict the magnitude of alpha/beta power decreases during subsequent retrieval. *Neuropsychologia* **153**, 107755 (2021).

40. Koenig, T., Studer, D., Hubl, D., Melie, L. & Strik, W. K. Brain connectivity at different time-scales measured with EEG. *Philos. Trans. R. Soc. B Biol. Sci.* **360**, 1015–1024 (2005).

41. Raichle, M. E. *et al.* A default mode of brain function. *Proc. Natl. Acad. Sci.* **98**, 676–682 (2001).

42. Snyder, A. Z. & Raichle, M. E. A brief history of the resting state: The Washington University perspective. *NeuroImage* **62**, 902–910 (2012).

43. Antonova, E. *et al.* EEG microstates: Functional significance and short-term test-retest reliability. *Neuroimage Rep.* **2**, 100089 (2022).

44. Zanesco, A. P., King, B. G., Skwara, A. C. & Saron, C. D. Within and between-person correlates of the temporal dynamics of resting EEG microstates. *NeuroImage* **211**, 116631 (2020).

45. Pipinis, E. *et al.* Association Between Resting-State Microstates and Ratings on the Amsterdam Resting-State Questionnaire. *Brain Topogr.* **30**, 245–248 (2017).

46. Tarailis, P., Šimkutė, D., Koenig, T. & Griškova-Bulanova, I. Relationship between Spatiotemporal Dynamics of the Brain at Rest and Self-Reported Spontaneous Thoughts: An EEG Microstate Approach. *J. Pers. Med.* **11**, 1216 (2021).

47. Croce, P., Zappasodi, F. & Capotosto, P. Offline stimulation of human parietal cortex differently affects resting EEG microstates. *Sci. Rep.* **8**, 1287 (2018).

48. Bréchet, L. *et al.* Capturing the spatiotemporal dynamics of self-generated, task-initiated thoughts with EEG and fMRI. *NeuroImage* **194**, 82–92 (2019).

49. Buckner, R. L., Andrews-Hanna, J. R. & Schacter, D. L. *The Brain's Default Network*: *Anatomy, Function, and Relevance to Disease*. *Ann. N. Y. Acad. Sci.* **1124**, 1–38 (2008).

50. Menon, V. 20 years of the default mode network: A review and synthesis. *Neuron* **111**, 2469–2487 (2023).

51. De Voogd, L. D. & Phelps, E. A. A cognitively demanding working-memory intervention enhances extinction. *Sci. Rep.* **10**, 7020 (2020).

52. Spielberger, C. D. Manual for the state-trait anxiety inventory (self-evaluation questionnaire).(No Title). (1970).

53. Beck, A. T., Steer, R. A., Epstein, N. & Brown, G. Beck Self-Concept Test. *Psychol. Assess. J. Consult. Clin. Psychol.* **2**, 191–197 (1990).

54. Boddez, Y. *et al.* Expectancy bias in a selective conditioning procedure: Trait anxiety increases the threat value of a blocked stimulus. *J. Behav. Ther. Exp. Psychiatry* **43**, 832–837 (2012).

55. Browning, M., Behrens, T. E., Jocham, G., O'Reilly, J. X. & Bishop, S. J. Anxious individuals have difficulty learning the causal statistics of aversive environments. *Nat. Neurosci.* **18**, 590–596 (2015).

56. Braithwaite, J. J., Watson, D. G., Jones, R. & Rowe, M. A guide for analysing electrodermal activity (EDA) & skin conductance responses (SCRs) for psychological experiments. *Psychophysiology* **49**, 1017–1034 (2013).

57. Society for Psychophysiological Research Ad Hoc Committee on Electrodermal Measures. Publication recommendations for electrodermal measurements. *Psychophysiology* **49**, 1017–1034 (2012).

58. Oostenveld, R., Fries, P., Maris, E. & Schoffelen, J.-M. FieldTrip: Open Source Software for Advanced Analysis of MEG, EEG, and Invasive Electrophysiological Data. *Comput. Intell. Neurosci.* **2011**, 1–9 (2011).

Figures

Figure 1

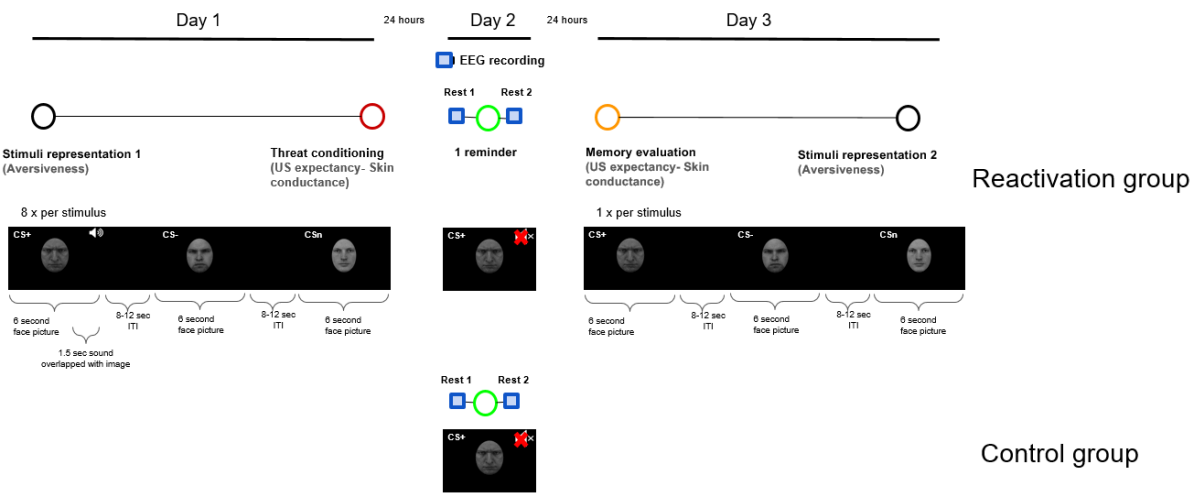

Figure 1. Schematic depiction of the experimental design illustrating group specifications across the three experimental sessions. Chronological outline of the experimental schedule for the two groups: Reactivation Group: performed the tasks across all three days, with a reminder of the CS previously paired with the US presented on the second day. Control Group: performed only the second-day task, observing the same reminder, but for them, it was the first time encountering it.

Figure 2

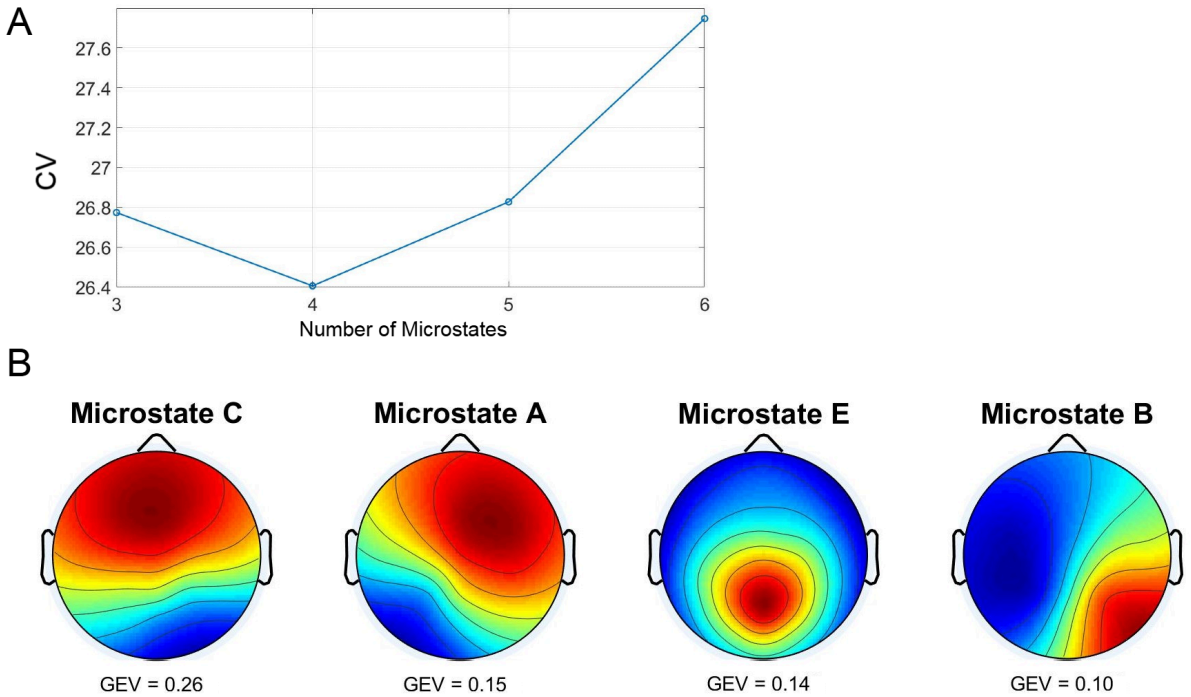

Figure 2. A) The CV was calculated for 3, 4, 5, and 6 Microstates, yielding an optimal number of 4 Microstates that minimized the CV. These are presented in B) Microstate prototypes ordered in decreasing GEV. They were labeled as C, A, E, and B according to Tarailis et al. (2024).

Figure 3

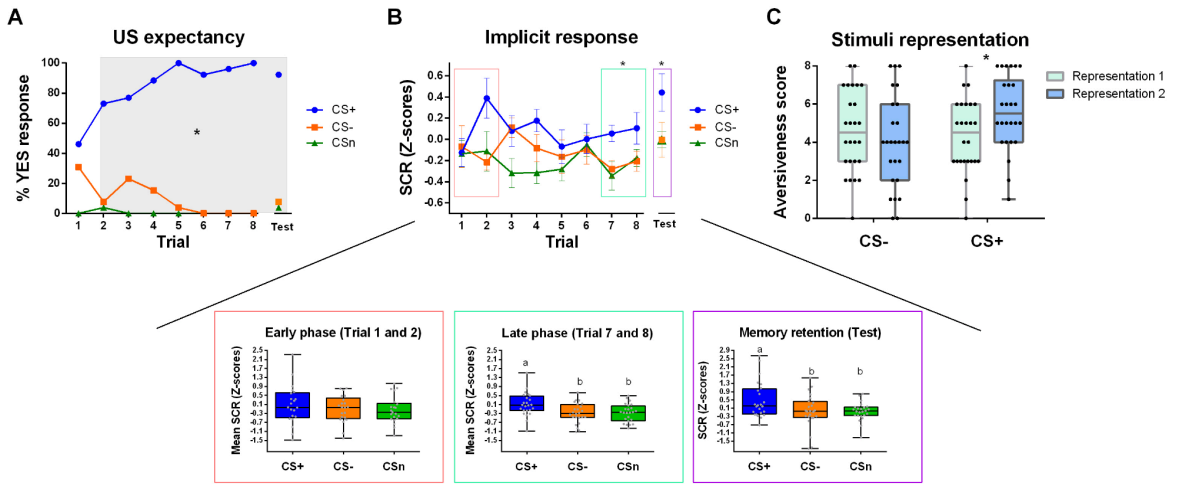

Figure 3. A) US expectancy represented as the proportion of “Yes” responses (“I will hear the tone after the CS”) for the three stimuli (CS+, CS–, CSn) across the eight conditioning trials and the test trial, 48 h later. B) Skin Conductance Response (z-scored) for the three stimuli (CS+, CS–, CSn) across the eight conditioning trials and the test trial, 48 h later. Boxplot of SCR (z-scored) for the early phase of conditioning (Trials 1–2), the late phase (Trials 7–8), and the test trial. Boxes represent the interquartile range, the line indicates the median, whiskers the minimum and maximum values, and each dot corresponds to each individual. Different letters indicate significant differences.
C) Boxplot of stimulus ratings (aversiveness score) before conditioning (Rating 1) and after conditioning (Rating 2) for CS– and CS+. Boxes represent the interquartile range, the line indicates the median, whiskers the minimum and maximum values, and each dot corresponds to each individual. Asterisks indicate significant differences.

Figure 4

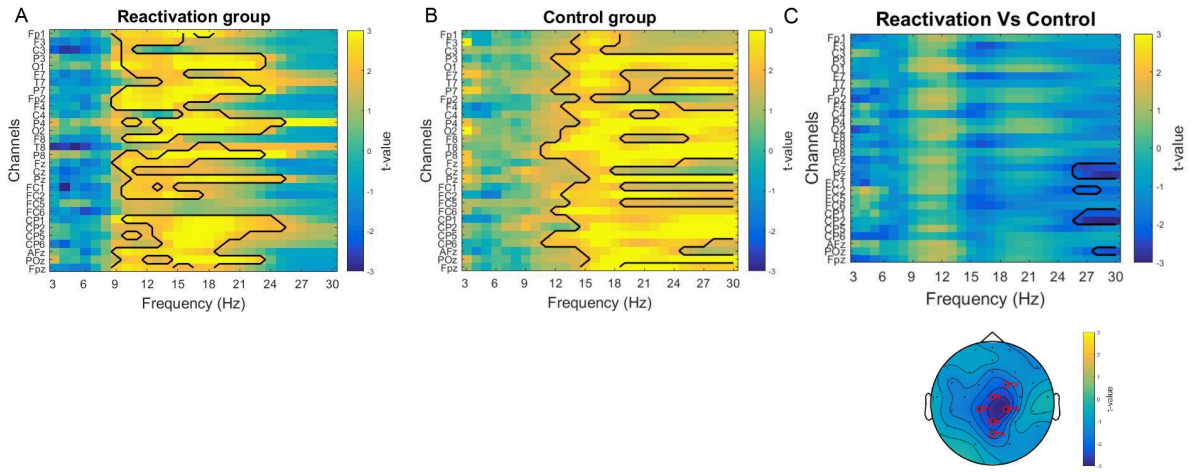

Figure 4. A) t-values from the cluster-based permutation test between Rest 2 and Rest 1 for the Reactivation and Control groups across all channels and frequencies (3–30 Hz). Contours indicate the significant positive cluster for each group.
B) t-values from the cluster-based permutation test of Rest 2 (baseline-corrected to Rest 1) between Reactivation and Control groups, restricted to the frequencies and channels where a significant

negative cluster was found in the between-group comparison. Topoplot shows the spatial distribution of significant channels and the corresponding t-values.

Figure 5

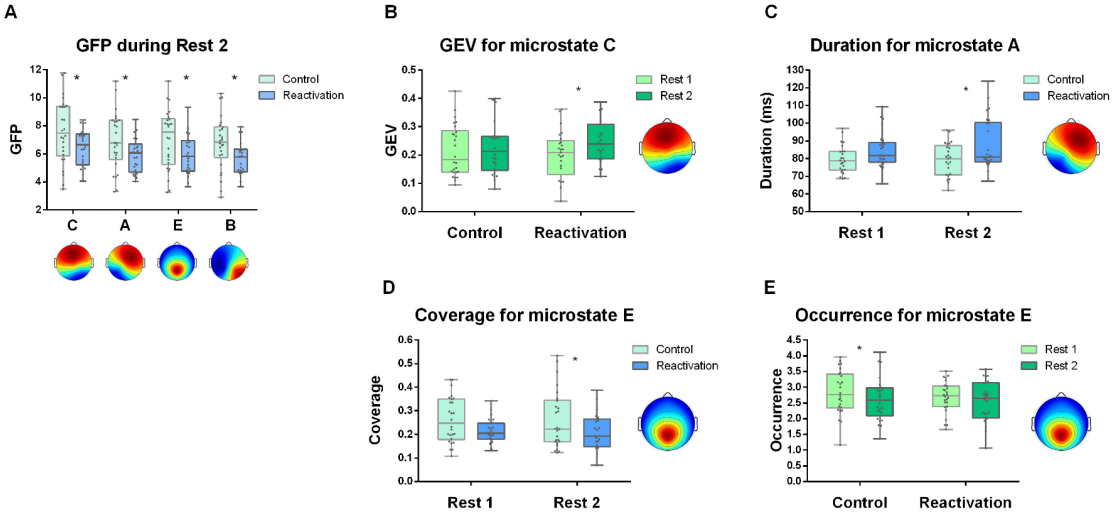

Figure 5. Boxplots showing interquartile range (boxes), median (line), minimum and maximum (whiskers), and individual values (dots) for: A) GFP for the 4 Microstates identified in the Reactivation and Control groups. Asterisks indicate significant differences between experimental groups.
B) GEV for Microstate C comparing Rest 1 and Rest 2 in both experimental groups. Asterisks indicate significant differences between resting states. C) Duration (ms) for Microstate A in each experimental group during Rest 1 and Rest 2. Asterisks indicate significant differences between experimental groups. D) Coverage for Microstate E in each experimental group during Rest 1 and Rest 2. E) Occurrence for Microstate E comparing Rest 1 and Rest 2 in both experimental groups. Asterisks indicate significant differences between experimental groups and between resting states, respectively.

Figure 6

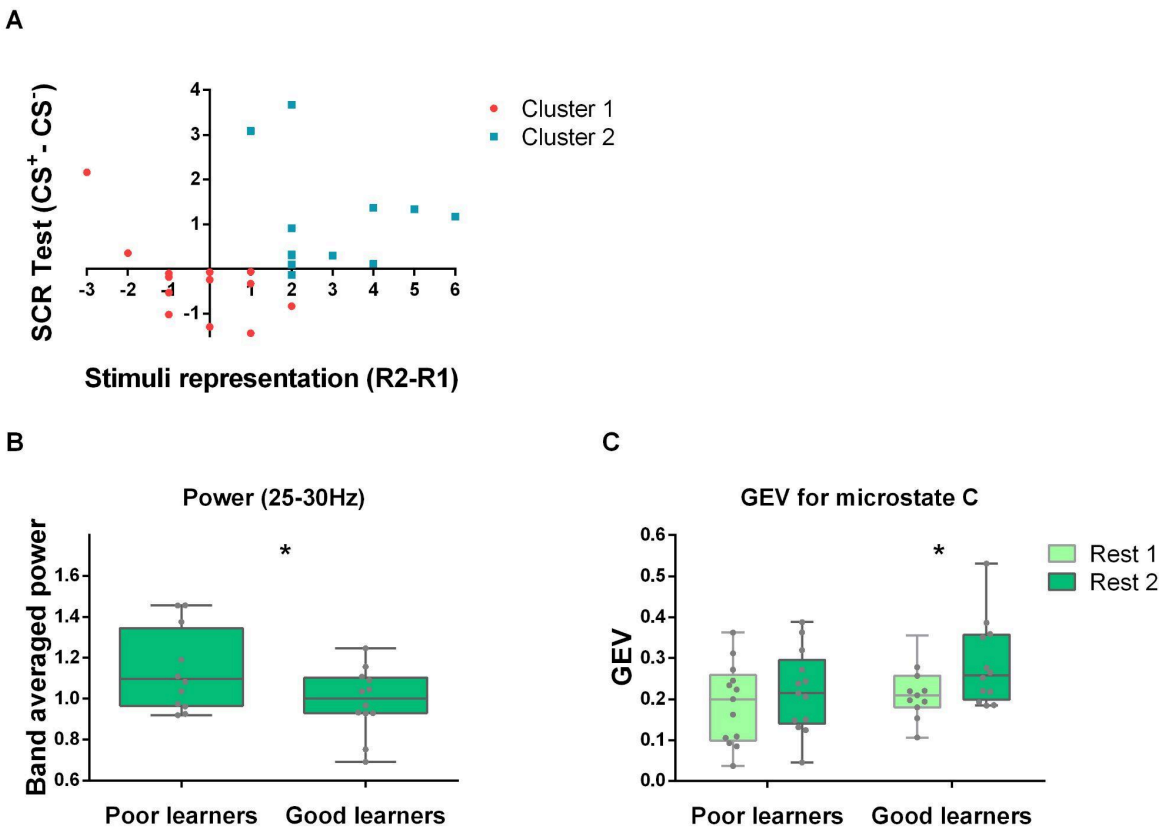

Figure 6. a) Participants were classified into two subgroups using k-means clustering (k = 2) based on standardized differences in evaluative scores and skin conductance responses (CS+ minus CS−) during testing. Cluster 1 was characterized as Poor learners, and cluster 2 was characterized as Good learners. b) Power for the significant electrodes found in figure 4C for 25-30 Hz, comparing Rest 2/Rest1 in Poor and Good learners. Asterisks indicate significant differences between resting states. c) GEV for Microstate C comparing Rest 1 and Rest 2 in Poor and Good learners. Asterisks indicate significant differences between resting states.

Supplementary material

Supplementary Figure 1. A) Twelve different male faces (seven angry and five neutral) were presented on a screen with a 0–8 aversiveness scale; one of the faces is shown as an example.

CS-	CSn	CS+	CS-	CS+	CS-	CSn	CS+	CSn	CS-	CSn	CS+	CS+	CSn	CS-	CS+	CS-	CSn	CS+	CS-	CSn	CSn	CS+	CS-
CS-	CS+	CSn	CS-	CS-	CSn	CS+	CS-	CS+	CSn	CSn	CS-	CS+	CSn	CS+	CS-	CSn	CS-	CS+	CS+	CSn	CS-	CSn	CS+
CSn	CSn	CS-	CS+	CSn	CS+	CS-	CSn	CS-	CS+	CS-	CSn	CS-	CS+	CSn	CS+	CS-	CS+	CSn	CS+	CS-	CS+	CSn	CS-
CS-	CSn	CS+	CS-	CS+	CSn	CS+	CS-	CSn	CS-	CS+	CSn	CS+	CS-	CSn	CS+	CSn	CS-	CS+	CSn	CS-	CS-	CS+	CSn

Supplementary Figure 2. During acquisition, each face was presented eight times in a different order. Four different combinations were used. The CS+ in red corresponds to the CS+ not paired with the US.

	acquisition	Test statistic	P-value
Shapiro-Wilk normality test	Early phase	w=0.97	p-value=0.367
Mauchly test for sphericity	Early phase	0.78	p-value=0.097
Levene`s test for homogeneity of variance	Early phase	f-value= 1.12	p-value=0.33
Shapiro-Wilk normality test	Late phase	w=0.97	p-value=0.472
Mauchly test for sphericity	Late phase	0.93	p-value=0.474
Levene`s test for homogeneity of variance	Late phase	f-value= 0.24	p-value=0.78
	Memory test		
Shapiro-Wilk normality test	Test	w=0.95	p-value=0.082
Mauchly test for sphericity	Test	0.96	p-value=0.708
Levene`s test for homogeneity of variance	Test	f-value= 2.58	p-value=0.082

Supplementary Table 1. Test statistics and p-values for the assumptions of the implicit response during the early and late phases of acquisition and the memory retention test.

Variable	Test	Likelihood Ratio Test	p-value
Time and Stimulus	Multicollinearity VIF=1		
Time	Proportional odds assumption	10.57	0.158

Stimulus	Proportional odds assumption	7.20	0.074

Supplementary Table 2. Test statistics and p-values for the assumptions of cognitive biases. Variance Inflation Factors (VIFs) are reported for the multicollinearity assumption, and the likelihood ratio test (LRT) and p-values are reported for the proportional odds assumption

Microstate		Estimate	SE	t-value	p-value
C	GFP rest1	0.93	0.52	(58)=1.78	0.083
A	GFP rest1	0.72	0.48	(57)=1.5	0.130
E	GFP rest1	0.78	0.52	(58)=1.5	0.139
B	GFP rest1	0.69	0.43	(60)=1.6	0.116

Supplementary Table 3. Test statistics and p-values for the comparison of Global Field Power between the Reactivation and Control groups during Rest 1.

Microstate	GEV Control	Estimate	SE	t-value	p-value
A	R1 vs R2	0.0073	0.0055	(43)=1.3	0.194
E	R1 vs R2	-0.0035	0.0069	(47)=-0.5	0.57
B	R1 vs R2	-0.0076	0.0046	(47)=-1.63	0.108
Microstate	GEV Reactivation	Estimate	SE	t-value	p-value
A	R1 vs R2	0.0024	0.0061	(45)=0.399	0.691
E	R1 vs R2	0.0034	0.0074	(47)=0.46	0.643
B	R1 vs R2	-0.0017	0.0047	(47)=-0.37	0.708

Microstate	Duration R1	Estimate	SE	t-value	p-value
C	Control vs Reactivation	5.08	7.00	(61)=0.72	0.47
E	Control vs Reactivation	5.51	4.09	(67)=1.348	0.18
B	Control vs Reactivation	0.33	2.46	(77)=0.135	0.892
Microstate	Duration R2	Estimate	SE	t-value	p-value
C	Control vs Reactivation	4.04	7.02	(62)=0.57	0.56
E	Control vs Reactivation	6.48	4.06	(67)=1.59	0.115
B	Control vs Reactivation	-0.32	2.46	(77)=-0.13	0.897

Microstate	Coverage R1	Estimate	SE	t-value	p-value
C	Control vs Reactivation	0.0036	0.029	(62)=0.125	0.9
A	Control vs Reactivation	-0.026	0.018	(62)=-1.42	0.15
B	Control vs Reactivation	-0.019	0.015	(61)=-1.26	0.21

Microstate	Coverage R2	Estimate	SE	t-value	p-value
C	Control vs Reactivation	-0.0067	0.029	(62)=-0.22	0.81
A	Control vs Reactivation	-0.036	0.018	(62)=-1.92	0.06
B	Control vs Reactivation	-0.008	0.015	(62)=-0.53	0.59

Microstate	Occurrence Control	Estimate	SE	t-value	p-value
C	R1 vs R2	-0.03	0.09	(50)=2.42	0.019
A	R1 vs R2	0.219	0.0069	(47)=-0.5	0.57
B	R1 vs R2	0.04	0.078	(50)=0.56	0.57
Microstate	Occurrence Reactivation	Estimate	SE	t-value	p-value
C	R1 vs R2	0.2	0.09	(50)=2.21	0.03
A	R1 vs R2	0.0034	0.0074	(47)=0.46	0.643
B	R1 vs R2	0.113	0.07	(50)=1.44	0.15

Supplementary Table 4. Test statistics and p-values for the remaining Microstate comparisons not shown in the main text.

Microstate	GFP	Group	Estimate	SE	t-value	p-value
C	R1 vs R2	Poor	-0535	0.23	(23)=-2.27	0.032
C	R1 vs R2	Good	-0.32	0.265	(23)=-1.2	0.24

Supplementary Table 5. Test statistics and p-values for the comparison of GFP between the Rest1 and Rest2 for Poor and Good learners group.